JOURNAL OF VIROLOGY, Apr. 2005, p. 4407–4414 Vol. 79, No. 7
0022-538X/05/$08.00+0 doi:10.1128/JVI.79.7.4407–4414.2005

Internal Point Mutations of the Capsid Modify the Serotype of *Rice Yellow Mottle Virus*

Eugénie Hébrard,[1]* Agnès Pinel-Galzi,[1] Vincent Catherinot,[2] Gilles Labesse,[2] Christophe Brugidou,[1] and Denis Fargette[1]

Institut de Recherche pour le Développement (IRD),[1] and Centre de Biochimie Structurale, CNRS UMR5048-INSERM U554, Faculté de Pharmacie,[2] Montpellier, France

Received 1 July 2004/Accepted 21 October 2004

Rice yellow mottle virus **is classified in five major serotypes; the molecular diversity of the coat protein (CP) is well established, but the amino acids involved in the recognition by discriminant monoclonal antibodies (MAbs) remain unknown. Reconstruction of a phylogenetic tree and sequence alignment of the CP gene of a sample representative of the continental-large diversity were used to identify 10 serospecific amino acids (i.e., conserved in all isolates belonging to the same serotype and distinct in other serotypes). Positions occupied by serospecific residues were localized on the crystal structure of the CP monomer and on modeled capsomers. Structural, molecular, and serological properties of each serotype were analyzed, and subsequently, hypotheses on the potential role of amino acids in discriminating reactions with antibodies were formulated. The residues 114 and 115 (serospecific of Sr1) and 190 (serospecific of Sr2) were localized on the outer surface of the capsid and might be directly involved in the immunoreactivity with MAb D and MAb A, respectively. In contrast, residues 180 (Sr3) and 178 (Sr5) lay within the inner surface of the capsid. To understand the role of these internal positions in the recognition with the antibodies, two substitutions (T180K and G178D) were introduced in the CP of an infectious clone. These mutations modified the antigenicity with MAb G and MAb E discriminating Sr3 and Sr5, respectively, while the reaction with MAb D remained unaffected. This result suggests an indirect effect of these two internal mutations on local immunostructure while the global structure was maintained.**

Antibodies have been used for a long time to detect, to identify, and to analyze the diversity of a large range of viruses. When directed against the nonenveloped viruses, the antibodies generally recognize the proteins which are the most exposed at the surface of the virions: the coat proteins (CP). To understand the specificity of such antibodies, the viral residues involved in recognition have to be identified. Several methods can be used to study it, in particular, the binding of monoclonal antibodies (MAbs) (which ensure an investigation of only one epitope at a time) with related viruses presenting known amino acid substitutions (29). In several well-documented cases, a single substitution was found to entirely abolish serological recognition by monoclonal antibodies. When substitutions are localized on surface-exposed zones of the capsid, they are expected to modify epitopes and to directly affect binding of the antibodies. Alternatively, amino acid substitutions can be localized at the surface of dissociated coat protein subunits; they belong to cryptotopes that are exposed in some instances during the serological assay (2, 4). Finally, some of these amino acids could be localized on the internal side of the capsid or of the coat protein (CP). In this case, they would have an indirect influence on the antigenic reactivity by altering the conformation of a distal surface-exposed antigenic region of the molecule (3, 8). When several substitutions differentiate two serotypes, the precise role of each amino acid change might be questioned. Correlated mutations can be analyzed in view of the capsid structure (when it is known).

In this publication, we assessed whether substitutions internal to the capsid can affect the antigenicity of the virus. We used *Rice yellow mottle virus* (RYMV) as a model, taking advantage of its clear-cut and correlated patterns of serological and molecular diversity (10) and of the resolution of its coat protein structure (22).

RYMV is one of the most important emergent plant viruses and is a threat to rice cultivation in Africa (1). Isolates representative of all the geographic zones where the disease is present have been collected, and their variability has been analyzed. RYMV diversity was first apparent from the detection of several serotypes in immunological studies with polyclonal and monoclonal antibodies (13, 14, 17, 18). Subsequently, five major serotypes (named Sr1 to Sr5) were defined using a set of discriminant monoclonal antibodies. Molecular typing of the coat protein through sequencing defined five major strains (named S1 to S5) and further identified several variants within each serotype (11). The phylogenetic tree inferred from the sequences had a characteristic nested structure with an East-to-West orientation of the clades, the most basal ones originating from East Africa possessing the highest nucleotide diversity.

RYMV is a single-stranded, positive-sense RNA sobemovirus (for a review on sobemoviruses, see reference 26). The CP of RYMV is encoded by open reading frame 4 (ORF4) from a subgenomic RNA, and its maximal nucleotide diversity reached 15% (10). RYMV possesses an icosahedral capsid made of 180 CP subunits assembled according to a T=3 qua-

* Corresponding author. Mailing address: IRD BP 64501, 34394 Montpellier cedex 5, France. Phone: 33 4 67 41 62 89. Fax: 33 4 67 41 62 83. E-mail: hebrard@mpl.ird.fr.

sisymmetry. The CP subunits fold into jelly roll β sandwiches, which is common in icosahedral viruses. The sobemovirus specificity is the presence of two extended loops between β-strands βG/βH and βF/βG (28). CP subunits adopt slightly different conformations depending on their position relative to the symmetry axes. A-type subunits cluster about the fivefold axes, whereas sets of three B-type and three C-type subunits cluster about quasi-sixfold axes. Beside the disordered 49 residues of the N terminus, 189 residues are visible in the subunits in the A and B positions. In the C-type subunits, part of the N terminus is ordered (residues 27 through 49), forming an additional β-strand named the βA arm. The βA arm is necessary for the T=3 assembly of *Sesbania mosaic virus* (16). The positions of βA arms on the inner surface of the capsid are different depending on the sobemovirus considered (22, 27). Compared to *Southern cowpea mosaic virus*, 3D swapping of strand βA around quasisixfold axes provides higher stability, under pressure and elevated pH, to RYMV.

In this article, serospecific amino acids (i.e., conserved in all isolates of the same serotype and different in any other serotype) were identified through parsimony analyses and comparison of the amino acid CP sequence alignments with the serological profiles of the isolates. Subsequently, the amino acid exchanges associated with changes in MAb recognition were identified. The positions of the serospecific amino acids were localized on the crystal structure of the CP monomer. The capsomers of each serotype were modeled in order to distinguish between the solvent-accessible positions (at the surface of the virion and/or at the surface of the monomers) and those buried. Putative effects (stability, conformational rearrangement, etc.) due to the sequence differences were analyzed at this stage. By directed mutagenesis of an infectious clone, we mutated two serospecific internal positions. We checked that these mutations modified serological binding by their respective MAbs and did not alter the recognition by the others. We proposed that these internal mutations induce structural modifications that are propagated distally, thus resulting in the local disruption of effective interactions between epitopes and monoclonal antibodies. The structural changes involved are discussed.

MATERIALS AND METHODS

Viral isolates. Analysis was conducted with a sample of 12 RYMV isolates collected from cultivated rice of different countries and agroecological zones, previously described in reference 10, to be representative of the viral diversity in Africa (Table 1). All the field isolates were inoculated on the susceptible *Oryzae sativa* cultivar IR64 to increase virus concentration as described in reference (12). The virus induced the characteristic yellow discoloration and mottling of leaves.

Immunological characterization. The serological properties of the 12 isolates of the collection were tested with a set of four monoclonal antibodies (MAb D, A, G, and E) directed against RYMV-Mg1 in triple-sandwich enzyme-linked immunosorbent assay (TAS-ELISA) as described in reference 18. The RYMV isolates were assigned to one of the five serological profiles encountered (Table 2).

Sequence analysis and identification of serospecific amino acids. The genomes of the 12 isolates were previously fully sequenced; they represent the genetic diversity of RYMV, i.e., each strain (10). The identification numbers of the sequences from the EMBL or GenBank databases are listed in Table 1. Two additional isolates, named CI8 and Tz18, were used in this analysis to complement the sample. The sequence of the isolate CIb used to resolve the CP structure was included in the sample. The sequences were aligned using CLUSTAL W with default parameters. The phylogenetic trees were reconstructed by parsimony analyses as implemented in PAUP version 4.10. Parsimony analyses and comparison of the amino acid CP sequence alignments with the serological profiles of the isolates allowed the identification of serospecific amino acids, i.e., conservation in all isolates belonging to the same serotype and distinct in other serotypes.

TABLE 1. Origins of the RYMV isolates

Isolate[a]	Strain	Country	Database no.
CIa	S3	Ivory Coast	AJ608206
CIb[b]	S1/AO		L20893
CI4	S1/AO		AJ608207
CI8	S2		AJ279909
CI63	S2		AJ608208
Ma10	S1/AO	Mali	AJ608209
Mg1	S4	Madagascar	AJ608211
Mg2	S4		AJ608212
Ni1	S1/AC	Nigeria	AJ608213
Ni2	S1/AC		AJ608214
SL4	S3	Sierra Leone	AJ608215
Tz3	S5	Tanzania	AJ608216
Tz5	S4		AJ608217
Tz8	S4		AJ608218
Tz18	S6		AJ877020

[a] All sequences were deposited in the EMBL database except the CIb isolate, which was deposited in GenBank.
[b] Isolate used to resolve the coat protein structure.

Validation of the presence of serospecific residues. The CP gene sequence of a second sample of 152 isolates was determined as described by Pinel (21). Briefly, genome fragments with the CP gene and part of the 3′ untranslated region were transcribed and amplified by reverse transcription-PCR after extraction of total RNA from leaves as described previously (5, 21). Sequencing was performed by using the *Taq* terminator sequencing kit (Applied Biosystems) with primers described previously (21) and analyzed on an Applied Biosystems 373A sequencer. Sequences were assembled and analyzed using Lasergene software by DNASTAR (SeqMan EditSeq). The sequences were aligned using CLUSTAL W with default parameters. The presence of the serospecific residues was validated.

Protein structural analysis. The crystal structure of RYMV (PDB1F2N) corresponds to the isolate CIb. The coordinates of the complete RYMV capsid were obtained in the PQS Protein Quaternary Structure database (http://pqs.ebi.ac.uk/). RYMV trimers, pentamers, and hexamers of each serotype were modeled with MODELLER (23), and the models were evaluated with the programs Verify3D (9) and PROSA (25). Sequence-structure alignment analysis, structure

TABLE 2. Serological profiles of the RYMV isolates assessed with MAbs in TAS-ELISA tests

Serotype	Code	MAb[c]			
		D	A	G	E
Sr1	Cl4[a]	0	4	4	4
	Ma10	0	4	4	4
	Ni1	0	4	4	4
	Ni2	0	4	4	4
Sr2	Cl8	4	0	4	4
	Cl63[a]	4	0	3	3
Sr3	CIa[a,b]	4	0	2	4
	SL4	3	2	1	1
Sr4	Mg1[a]	4	4	4	4
	Mg2	4	4	4	4
	Tz5	4	4	4	4
	Tz8	4	4	4	4
Sr5	Tz3[a]	4	4	4	0
	Tz18	3	4	2	0

[a] Isolates chosen to model the structure of one capsomer of each serogroup.
[b] Infectious clone.
[c] Absorbances were coded as follows: "0" ≤ 0.30; 0.31 ≤ "1" ≤ 0.60; 0.60 < "2" ≤ 1.20; 1.20 < "3" ≤ 1.80; 1.80 < "4".

superpositions, and three-dimensional (3D) manipulations were done through visualization using ViTO (7; http://abcis.cbs.cnrs.fr/vito).

Coat protein gene mutations. Mutations were introduced into an infectious RYMV full-length cDNA (clone FL5 originated from isolate CIa cloned downstream of the T7 promoter) (5). Two nonsynonymous point substitutions in the RYMV coat protein cistron at nucleotides 3982 and 3988 (amino acids 178 and 180, respectively) were generated in two mutated clones named FL5-CPT180K and FL5-CPG178D, respectively. FL5 DNA was used as a template for amplification in PCR with the forward primer R15B (5′-TTATGAACTCTGTTTTC C-3′) corresponding to the FL5 sequence (nucleotides 2991 through 3008) and a reverse primer RCPG178D (5′-AATGGA*ACTAGT*AACGCGTGTCCAG**T**CA C-3′) or RCPT180K (5′-AATGGA*ACTAGT*AACGCGT**T**TCCAGCCAC-3′) containing the restriction site SpeI (italics) and the point mutations at G178D and T180K (boldface), respectively. The reaction mixture contained 0.02 U of DyNAzyme EXT DNA polymerase (Finnzymes-Ozyme) in appropriate buffer, 10 μmol of dNTP, and 30 pmol of forward and reverse primer. After denaturation of DNA at 94°C for 3 min, the reaction mixture was subjected to 30 cycles of 30 s at 94°C, 30 s at 53°C, and 1 min at 72°C. The PCR fragments were incubated at 72°C for 10 min and stored at 4°C. After purification by using a Qiaquick PCR purification kit (QIAGEN), PCR products were double digested by NcoI (the restriction site is localized at position 3128) and SpeI (Biolabs) 2 h at 37°C in an appropriate buffer. Fragments were extracted by using a Qiaquick gel extraction kit (QIAGEN) and ligated with ligase (Promega) in an appropriate buffer overnight at 15°C into FL5 previously digested by NcoI and SpeI. Recombinant plasmids were transformed into competent *Escherichia coli* strain XLIBlue or DH5-α cells. Mutations were confirmed by sequencing each inserted fragment at least once in each sense with a set of primers.

In vitro transcription and plant inoculation of native and mutated clones. Plasmid DNAs, purified with the HiSpeed Plasmid Midi kit (QIAGEN), were digested with HindIII, which linearizes native and mutated FL5 at the 3′ end of the RYMV cDNA. In vitro transcriptions by T7 RNA polymerase (Promega) were done as described in reference 5. Susceptible IR64 plants were mechanically inoculated with a 1-μg/μl concentration of in vitro transcripts of infectious clones diluted in inoculation buffer (0.1 M KH_2PO_4 and 0.1 M Na_2HPO_4 adjusted to pH 7.2) and with carborundum.

RESULTS

Identification of serospecific amino acids. A phylogenetic tree was inferred from full-length sequences of isolates representative of the RYMV diversity (10) (Fig. 1). The tree was characterized by an East-to-West orientation of the clades, the most basal ones originating from East Africa. Isolates were serotyped with a set of four monoclonal antibodies (Table 2; Fig. 1). As expected, all monoclonal antibodies reacted against the homologous Sr4 isolates. Any other serotypes were characterized by the lack of reaction with one monoclonal antibody. The isolates of serogroup Sr1, Sr2, Sr3, and Sr5 were not recognized by MAb D, A, G, and E, respectively.

The clear-cut phylogenetic pattern of the tree, its pronounced nested structure, and the relationships between phylogenetic strains and serotypes allowed the identification of the nodes associated with MAb recognition, the identification in the coat protein of serospecific amino acids, and the corresponding changes leading to modification in serological recognition (Fig. 1). Lack of response of the Sr5 isolates with MAb E was correlated with an aspartic acid at position 178 in comparison to a glycine in the other serogroups D178G (node 1). Lack of detection of Sr1 isolates by MAb D was associated with three substitutions, A70S, A114T, and T115V (node 2). Lack of response of Sr2 isolates with MAb A was related to A190T (node 4). Abolition of reaction of Sr3 isolates with MAb G was consistent with N53K, K180T, I198 M, and/or I209V exchanges (node 4′).

The observation of the sequence alignment of the 15 isolates allowed the detection of an additional Sr5-specific residue

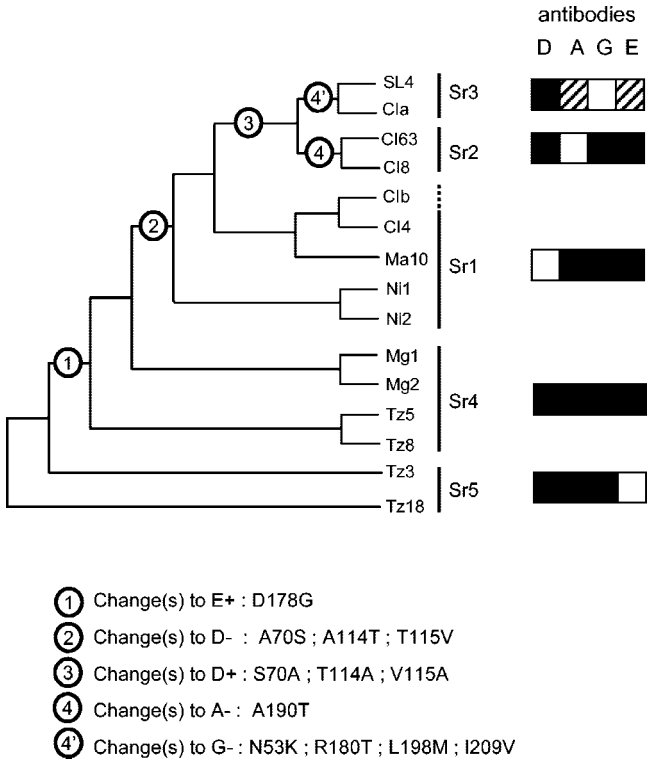

FIG. 1. Cladogram of 15 representative isolates inferred from maximum parsimony analysis of the full-length sequences. The serotypes of the isolates and their antigenic profile with the monoclonal antibodies are indicated at the right of the figure. The nodes associated with changes in MAb recognition are numbered on the cladogram. The corresponding serospecific changes are indicated at the bottom of the figure. The residue numbering was that of isolate CIb used to solve the CP three-dimensional structure.

which corresponded to an arginine inserted between the positions 59 and 60 (Fig. 2). The presence of these 10 serospecific residues was validated on the total corpus of 152 isolates (Table 3). There were very few exceptions: 1 Sr1 isolate out of 46 lacked S70, and 1 Sr2 isolate out of 48 lacked T190 (see Discussion).

3D localization of serospecific residues. The serospecific positions were localized on the crystal structure of the CP monomer (Fig. 3). None of these residues were buried within the core of the monomer formed by two sheets of four β-strands (labeled A to I), suggesting that the monomer structure would not be affected by these substitutions. The serospecific positions were observed to cluster at two opposite faces of the monomer. On one side, the positions 70, 114, 115, and 209 were localized within the loops connecting β-strands βB/βC, βD′/βE, and βH/βI, respectively. On the other side of the monomer, the positions 178, 180, 190, and 198 were localized between β-strands βG and βG′, at the beginning of βG′, at the beginning of the helix αE, and at the end of αE, respectively. Finally, the positions 53 and 59 were localized between β-strands βA/βB and in βB, respectively. Some positions related to the same serospecificity were observed at some distance from each other in the monomer (Sr3 and Sr5), while substitutions from distinct serotypes were observed in rather close proximity (Sr2, Sr3, and Sr5).

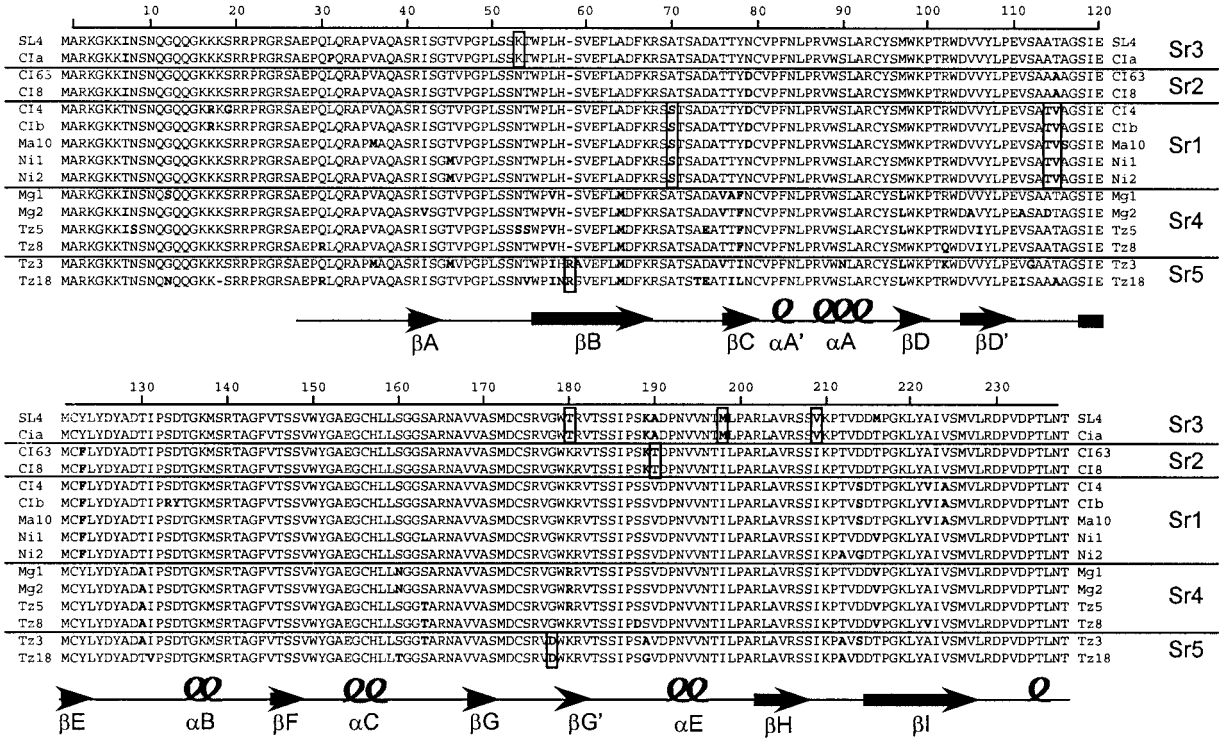

FIG. 2. Alignment of the amino acid sequences of the coat protein of 15 RYMV isolates. The sequences are listed in the same order as those in the phylogenetic tree. The serotypes are indicated at the right of the figure. For each variable position from the consensus sequence, differences of amino acids are boldface. The serospecific positions (amino acids conserved in all the isolates of one serogroup but different in the other serogroups) are boxed. The locations of β-sheets (black arrows) and the α-helices (black springs) are based on their positions in the X-ray crystal structure of RYMV CIb chain A.

Antibodies were not raised against the monomer but against virions purified from plants infected by the isolate Mg1 (18). A symmetry-related monomer may bring an equivalent residue in the vicinity of the other residues to form one epitope in the assembled capsid (called neotopes). In agreement, serospecific positions appeared to cluster around the quasi-threefold, the fivefold, and the quasi-sixfold axes (Fig. 4). The positions 178, 180, 190, and 198 were localized in the vicinity of the quasi-threefold axis like position 53 was. The positions 114 and 115 were localized near both the fivefold and the quasi-sixfold axes but were more accessible on the pentamer than on the hexamer (Fig. 6 and 7). The positions 59, 70, and 209 were localized around the quasi-sixfold axes. Positions 70, 114, 115, 190, and 209 were at the external surface of the capsid (Fig. 5 through 7). By contrast, the positions 53, 59, 198, 180, and 178 (serospecifics of Sr3 and Sr5) were buried at some distance from the capsomer outer surface and were not accessible to the solvent (Fig. 3 and 5). These observations raised the question of the role of each substitution on the recognition by the various MAbs. To characterize the influence of these residues on the structure of the capsid, we modeled one capsomer for one isolate of each serogroup. The models suggested that little conformational changes are to be expected for the monomer as well as for the capsomer (except for the substitution G178D, which is discussed in more detail below). Most models produced by MODELLER and evaluated using the programs Verify3D (9) and Prosa (25) appeared as good as (or even better than) the template structure (PDB1F2N). Indeed, no

TABLE 3. Validation of serospecific residues on the entire collection of CP sequences

Serotype	Substitutions	S1 (n = 46)	S2 (n = 48)	S3 (n = 9)	S4 (n = 24)	S5+S6 (n = 15)
Sr1	S70	45	0	0	0	1
	T114	46	1	0	0	0
	V115	46	1	0	0	0
Sr2	T190	0	47	0	0	0
Sr3	K53	0	0	9	0	0
	T180	0	0	9	0	0
	M198	0	0	9	0	0
	V209	0	0	9	0	0
Sr5	R59′	0	0	0	0	15
	D178	0	0	0	0	15

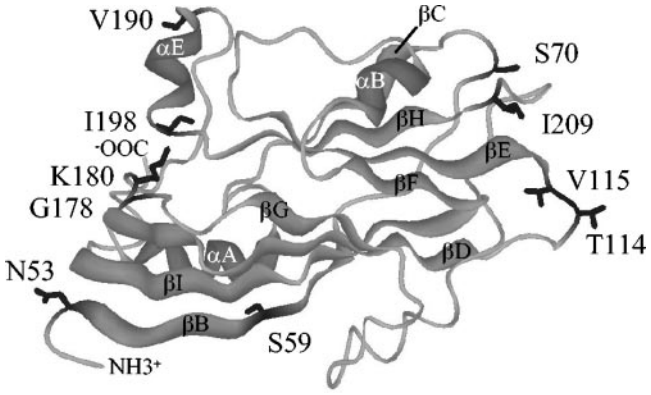

FIG. 3. Structure of the core of RYMV CP (PDB1F2N). The side chains of the serospecific residues are shown in black and labeled with their position numbers. β-Strands and α-helices are drawn as ribbons and labeled according to Qu et al. (22). N and C termini are labeled $NH3^+$ and COO^-, respectively. The positions 53, 178, 180, 190, and 198 are facing the quasithreefold axis. Figure was drawn using ViTO (7).

steric clashes were detected by structure visualization. Interaction with the close environment of each substitution suggested that little structural changes are necessary to accommodate the sequence change (or maybe compensate by the binding of dications in the case of the G178D substitution). Similarly, the nature of the amino acid was mostly compatible with the backbone conformation observed in the crystal structure at the substituted positions.

Internal amino acids influenced antibody recognition. In this analysis, the residues identified as serospecific were supposed to be involved in the absence of response with one monoclonal antibody. However, some of the serospecific substitutions (or insertions) may only be associated with the strain differences. Their causality should be checked by mutagenesis. We focused on the role of the internal ones.

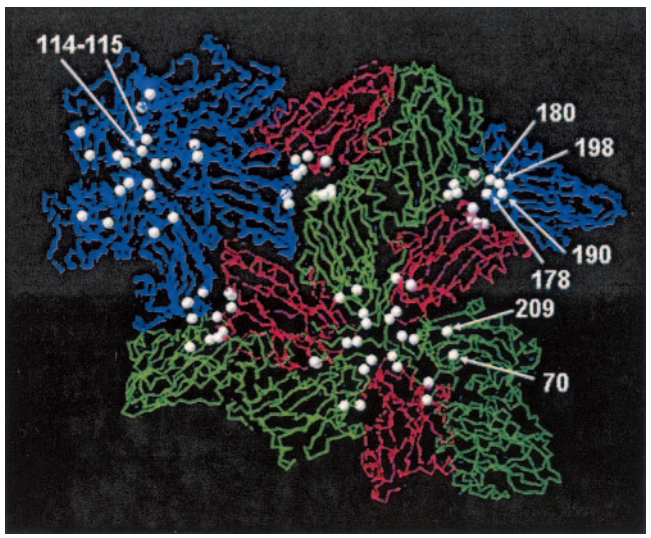

FIG. 4. Structure of the capsomer. A-type subunits are in blue, B-type subunits are in red, and C-type subunits are in green. White circles represent the serospecific amino acids (for clarity, positions 53 and 59 are not indicated).

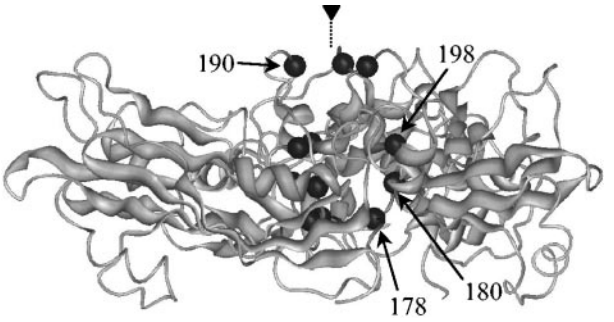

FIG. 5. Structure of the CP trimer. Black circles indicated the serospecific amino acids that are labeled according to their position. Position 190 is solvent exposed, while positions 178, 180, and 198 are buried at the trimer interface (see text). For clarity, position 53 is not indicated. The dashed arrow represents the quasithreefold axis.

Sr3 isolates were characterized in particular by the presence of internal T180 instead of a lysine (Fig. 8). To determine if T180 has an influence on the recognition with MAb G (discriminating Sr3), the infectious clone CIa belonging to Sr3 was mutated to create CIa CP T180K. The plants mechanically infected by the transcript of the mutated clone presented symptoms. No differences in infectivity were observed between the wild-type infectious clone CIa and its variants. Leaves were tested in TAS-ELISA. The serotype was identical to nonmutated CIa except that the reaction intensity with the monoclonal antibody G changed from 2 to 4 (Table 4). This suggested that the residue change altered the capsid structure only locally and modified neither the other epitopes nor the CP assembling.

Sr5 isolates were characterized in particular by the presence of internal D178 instead of a glycine (Fig. 9). We tested the influence of D178 on the recognition with MAb E (discriminating Sr5) replacing G178D in the infectious clone CIa. The mutated clone was infectious, and its serotype was identical to nonmutated CIa except that the reaction with the MAb E was abolished (the reaction intensity changed from 4 to 0) (Table 4). Again, a residue localized far from the outer surface of the capsid was shown to be involved in the serological responses.

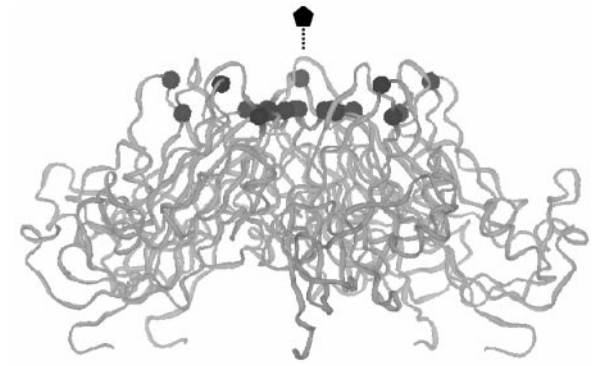

FIG. 6. Structure of the pentamer. Black circles indicated the serospecific amino acids (70, 114, 115, and 209). For clarity, position 59 is not indicated. The dashed line represents the fivefold axis.

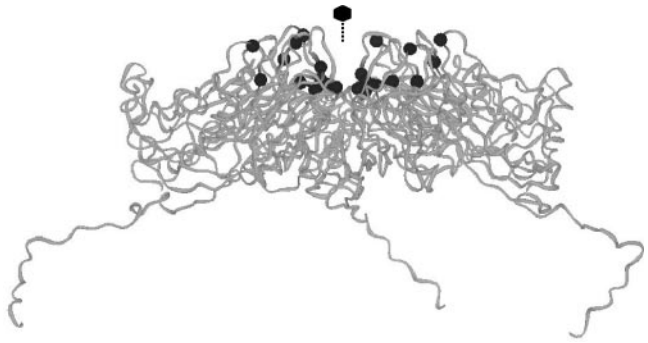

FIG. 7. Structure of the hexamer. Black circles indicated the serospecific amino acids (70, 114, 115, and 209). For clarity, position 59 is not indicated. The dashed line represents the quasisixfold axis.

DISCUSSION

The analysis of the molecular, serological, and structural data of a sample of 15 isolates representative of the RYMV diversity at a continent scale allowed us to formulate hypotheses on the amino acids involved in serological responses. We completed and refined the previous analysis (11). We identified 10 serospecific amino acids and validated them on the whole collection (152 isolates).

S70, T114, and V115 were specific to Sr1 characterized by the absence of recognition with MAb D. These residues were localized at the surface of the capsid. The analysis of an atypical isolate provided us with additional information. The isolate Gh1 belonged to S2 but possessed the serotype Sr1. Isolate Gh1 exhibited T114 and V115 like isolates of Sr1 but not S70, suggesting that S70 was not involved in the absence of response of MAb D discriminating Sr1. The crystallographic analyses of antigen-antibody complexes showed that the antibody was in contact with a 700- to 900-Å^2 area at the protein surface of the antigen (29). Because of their position at the fivefold and quasisixfold axes, the residues 114 and 115 formed an area of approximately 800 Å^2. Moreover, the absence of response with this MAb is associated with substitutions that modify the nature of the residues (in particular, the change at position 115 from polar to hydrophobic). The role of the electrostatic interactions involving, for example, alanine or threonine at the antigen-antibody binding site was previously demonstrated (24). We concluded that the residues 114 and 115 probably correspond to the epitope recognized by MAb D.

TABLE 4. Serological profiles of the RYMV infectious clones assessed with MAb in TAS-ELISA tests

RYMV	MAb[a]			
	D	A	G	E
CIa	4	0	2	4
CIa CP G178D	4	0	2	0
CIa CP T180K	4	1	4	4

[a] Absorbances were coded as follows: "0" ≤ 0.30; 0.31 ≤ "1" ≤ 0.60; 0.60 < "2" ≤ 1.20; 1.20 < "3" ≤ 1.80; 1.80 < "4".

Isolates of Sr2 were characterized by only one residue, T190, localized at the surface of the capsid near the quasi-threefold axis, suggesting that this position belongs to the epitope recognized by MAb A (Fig. 8). However, the atypical isolate S2/Sr1 Gh1 possesses T190 but reacts with MAb A. This unique exception might be due to the influence of other residues which might allow, in this case, the binding of the antibody despite the presence of T190. However, we cannot exclude the possibility that residue 190 does not belong to the epitope recognized by MAb A and that other non-Sr2-specific residues induce a folding incompatible with the binding of the antibody.

The situation of isolates of Sr3 was more complex because their specificity was made of four residues and the majority of them were not localized at the surface of the capsid. The small number of Sr3 isolates may explain this higher number of specific residues: some of them might be due to a bias of the sample and could not influence the serological response. We noticed that isolates of the Sr3 serotype were the most difficult to characterize. Responses with MAb A and E depended on the isolates. Serotyping experiments have to be repeated more times for these isolates. One explanation is that the Sr3 sero-

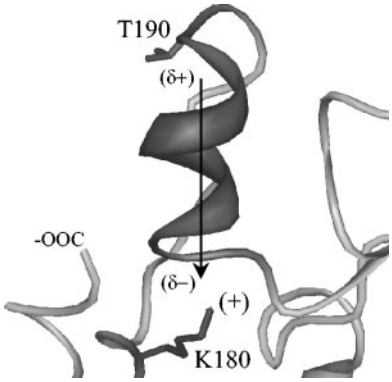

FIG. 8. Structural analysis of specific substitution in Sr2 and Sr3 around position 180. The side chains (for clarity, only K180 and T190 of Sr2 are illustrated) are shown in black and labeled with their position numbers. The macrodipole of the α-helix likely interacts favorably with the positively charged lysine, while the substitution by a short and uncharged threonine may destabilize this conformation and change the immunoreactivity (see text).

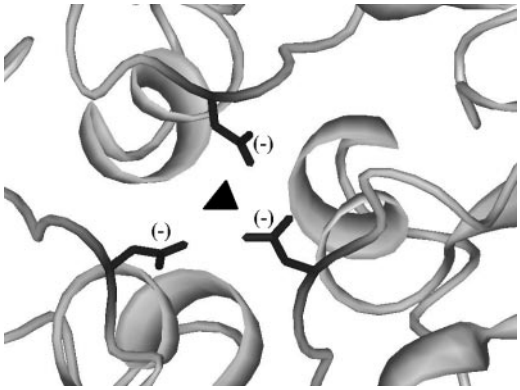

FIG. 9. Structural analysis of specific substitution in Sr2 and Sr5 around position 178. The putative orientations of the side chains of the serospecific aspartate D178 are shown in black according to the deduced model. The negatively charged aspartates point toward the quasithreefold axis. Their close proximity in space might form a new dication binding site as well as induce local rearrangement (see text).

type represents the group which has differentiated the most recently in the evolutionary history of RYMV (Fig. 1) (10). Consequently, it is very different from Sr4 which the isolate Mg1 belongs to and which was used to produce the monoclonal antibodies. In other words, the available MAbs are not the most appropriate to characterize Sr3 isolates. New MAbs directed against an isolate of the strain S3 or even S2 (which is the most similar strain to S3) would respond more strongly with isolates S3.

In this study, we demonstrated that the substitution of the internal T180 near the quasi-threefold axis was sufficient to enhance recognition with MAb G. This serospecific position corresponded to the most important change in amino acid nature. On the contrary, the external V209 (valine instead of the closely related isoleucine) was localized at the vicinity of the fivefold axis. K53 localized at the periphery of the trimer corresponded to a conservative change like I198M. The latter two amino acid positions might neither alter the structure of the capsid nor affect the recognition by MAbs.

Interestingly, the residue 180 was buried inside the capsid (Fig. 5 and 8). However, its substitution (T180K in a Sr3 context) significantly affected the recognition by only one antibody (MAb G) while the virus particle remained functional and was recognized by MAb D. Nevertheless, the change should propagate to the outer surface of the particle and alter the epitope structure or its conformational dynamic. The mutation T180K changed dramatically both the size and the charge of the amino acid side chain. According to our models, the positive charge of the lysine might favorably interact with the macrodipole of the α-helix E (residues 192 to 198). This may change the stability of the helix αE or its orientation, which in turn would change the conformation of the residues on the surface and affect the reaction with MAb G.

Finally, the isolates of Sr5 were characterized by the presence of R59′ and D178. We demonstrated that the substitution G178D was sufficient to abolish the recognition with MAb E, suggesting that the addition of an arginine after position 59 was not involved in the serotype. As was the case for position 180, the substitution of the buried G178 into an aspartate might indirectly change the conformation of the same surface-exposed epitope (Fig. 5 and 9). The distance between Cα of the three G178 related by the quasithreefold symmetry axis was 9 Å. Replacing these glycines by aspartic acids brought three negative charges at 6 Å from each other. With or without compensation by the binding of a dication such as calcium (or magnesium) (15) or reorientation of the aspartic side chains, the precise orientation of each CP monomer around the quasithreefold symmetry might be affected.

The hypothesis of direct recognition of the residues 178 and 180 by MAb G and E due to dissociation of the capsid in coat protein monomers was discarded on the following grounds. Indeed, RYMV is a highly stable icosahedral virus, in particular, because of the swapping of the βA arm and its ability to change from swollen form to compact form with calcium atoms (20, 22). We believe that even during a screening of MAbs by a DAS ELISA (which has been demonstrated to induce dissociation of the rod-shaped tobamovirus TMV [4]), the majority of the RYMV capsids remain intact (in agreement with the recognition by MAb D).

The majority of epitopes found in proteins are discontinuous, formed by 15 to 22 amino acids (29). The RYMV epitopes recognized by the monoclonal antibodies studied here contain residues belonging to several CP monomers. Indeed, in a spot scan analysis, peptides representing the CP sequence of a Sr4 isolate have not been recognized by MAb A and E (H. Halimi, personal communication). In conclusion, the results obtained support the existence of two areas representing neotopes. (i) One is recognized by MAb D, containing the residues 114 and 115 localized at the surface near the fivefold and quasisixfold axes. The antibody might react easily with these residues at the fivefold axis because they are more accessible in relation to the absence of the βA arm between monomers at this axis. (ii) Another recognized by MAb A, G, and E, containing the extremity of the loop (between βG′ and αE) and the helix αE.

These two areas corresponded, as expected, to protrusions at the surface of the RYMV capsid (20). Their accessible localization associated with their abilities to react with monoclonal antibodies suggested they could be good candidates for interaction with host cell proteins. Preliminary results of a proteomic analysis of the complex formed by the virus particle and rice proteins by using two-dimensional gel electrophoresis and mass spectrometry showed that the two areas interacted with plant proteins (J. P. Brizard and C. Brugidou, unpublished data). These interactions could be validated by competition experiments with appropriate MAbs.

The property of RYMV to swell has been suggested to play a biological role (6, 19). Isoforms (swollen or compact particles) are not localized in the same subcellular compartments. Compact forms could represent forms of storage and long-distance movement in xylem vessels. Serological assays with monoclonal antibodies could be a useful tool to better understand the modifications of structure during swelling and the biological functions associated.

ACKNOWLEDGMENTS

Helpful discussions with M.H.V. van Regenmortel, T. Lin, C. Fauquet, and B.D. Harrison and technical assistance of J. Aribi are gratefully acknowledged.

REFERENCES

1. **Abo, M. E., A. A. Sy, and M. D. Alegbejo.** 1998. Rice Yellow Mottle Virus (RYMV) in Africa: evolution, distribution, economic significance on sustainable rice production and management strategies. J. Sustainable Agric. **11:** 85–111.
2. **Al Moudallal, Z., D. Altschuh, J. P. Briand, and M. H. Van Regenmortel.** 1984. Comparative sensitivity of different ELISA methods for detecting monoclonal antibodies to viruses. Dev. Biol. Stand. **57:**35–40.
3. **Al Moudallal, Z., J. P. Briand, and M. H. Van Regenmortel.** 1982. Monoclonal antibodies as probes of the antigenic structure of tobacco mosaic virus. EMBO J. **1:**1005–1010.
4. **Altschuh, D., Z. Al Moudallal, J. P. Briand, and M. H. Van Regenmortel.** 1985. Immunochemical studies of tobacco mosaic virus–VI. Attempts to localize viral epitopes with monoclonal antibodies. Mol. Immunol. **22:**329–337.
5. **Brugidou, C., C. Holt, M. N. Yassi, S. Zhang, R. Beachy, and C. Fauquet.** 1995. Synthesis of an infectious full-length cDNA clone of rice yellow mottle virus and mutagenesis of the coat protein. Virology **206:**108–115.
6. **Brugidou, C., N. Opalka, M. Yeager, R. N. Beachy, and C. Fauquet.** 2002. Stability of rice yellow mottle virus and cellular compartmentalization during the infection process in Oryza sativa (L.). Virology **297:**98–108.
7. **Catherinot, V., and G. Labesse.** 2004. ViTO: tool for refinement of protein sequence-structure alignments. Bioinformatics **20:**3694–3696.
8. **Dore, I., D. Altschuh, Z. Al Moudallal, and M. H. Van Regenmortel.** 1987. Immunochemical studies of tobacco mosaic virus–VII. Use of comparative surface accessibility of residues in antigenically related viruses for delineating epitopes recognized by monoclonal antibodies. Mol. Immunol. **24:**1351–1358.
9. **Eisenberg, D., R. Luthy, and J. U. Bowie.** 1997. VERIFY3D: assessment of

protein models with three-dimensional profiles. Methods Enzymol. **277:**396–404.
10. **Fargette, D., A. Pinel, Z. Abubakar, O. Traoré, C. Brugidou, S. Fatogoma, E. Hébrard, M. Choisy, Y. Séré, C. Fauquet, and G. Konaté.** 2004. Inferring the evolutionary history of *Rice Yellow Mottle Virus* from genomic, phylogenetic, and phylogeographic studies. J. Virol. **78:**3252–3261.
11. **Fargette, D., A. Pinel, H. Halimi, C. Brugidou, C. Fauquet, and M. Van Regenmortel.** 2002. Comparison of molecular and immunological typing of isolates of Rice yellow mottle virus. Arch. Virol. **147:**583–596.
12. **Fargette, D., A. Pinel, O. Traoré, A. Ghesquière, and G. Konaté.** 2002. Emergence of resistance-breaking isolates of Rice yellow mottle virus during serial inoculations. Eur. J. Plant Pathol. **108:**585–591.
13. **Fauquet, C., and J. Thouvenel.** 1977. Isolation of the rice yellow mottle virus in Ivory Coast. Plant Dis. Rep. **61:**443–446.
14. **Konate, G., O. Traore, and M. M. Coulibaly.** 1997. Characterization of rice yellow mottle virus isolates in Sudano-Sahelian areas. Arch. Virol. **142:**1117–1124.
15. **Labesse, G., E. Garnotel, S. Bonnel, C. Dumas, J. M. Pages, and J. M. Bolla.** 2001. MOMP, a divergent porin from Campylobacter: cloning and primary structural characterization. Biochem. Biophys. Res. Commun. **280:**380–387.
16. **Lokesh, G. L., T. D. Gowri, P. S. Satheshkumar, M. R. Murthy, and H. S. Savithri.** 2002. A molecular switch in the capsid protein controls the particle polymorphism in an icosahedral virus. Virology **292:**211–223.
17. **Mansour, A. N., and K. W. Baillis.** 1994. Serological relationships among rice yellow mottle virus isolates. Ann. Appl. Biol. **125:**133–140.
18. **N′Guessan, P., A. Pinel, M. L. Caruana, R. Frutos, A. A. Sy, A. Ghesquiere, and D. Fargette.** 2000. Evidence of the presence of two serotypes of rice yellow mottle sobemovirus in Côte d'Ivoire. Eur. J. Plant Pathol. **106:**167–178.
19. **Opalka, N., C. Brugidou, C. Bonneau, M. Nicole, R. N. Beachy, M. Yeager, and C. Fauquet.** 1998. Movement of rice yellow mottle virus between xylem cells through pit membranes. Proc. Natl. Acad. Sci. USA **95:**3323–3328.
20. **Opalka, N., M. Tihova, C. Brugidou, A. Kumar, R. N. Beachy, C. M. Fauquet, and M. Yeager.** 2000. Structure of native and expanded sobemoviruses by electron cryo-microscopy and image reconstruction. J. Mol. Biol. **303:**197–211.
21. **Pinel, A., P. N′Guessan, M. Bousalem, and D. Fargette.** 2000. Molecular variability of geographically distinct isolates of Rice yellow mottle virus in Africa. Arch. Virol. **145:**1621–1638.
22. **Qu, C., L. Liljas, N. Opalka, C. Brugidou, M. Yeager, R. N. Beachy, C. M. Fauquet, J. E. Johnson, and T. Lin.** 2000. 3D domain swapping modulates the stability of members of an icosahedral virus group. Structure **8:**1095–1103.
23. **Sali, A., and T. L. Blundell.** 1993. Comparative protein modelling by satisfaction of spatial restraints. J. Mol. Biol. **234:**779–815.
24. **Sinha, N., S. Mohan, C. A. Lipschultz, and S. J. Smith-Gill.** 2002. Differences in electrostatic properties at antibody-antigen binding sites: implications for specificity and cross-reactivity. Biophys. J. **83:**2946–2968.
25. **Sippl, M. J.** 1993. Recognition of errors in three-dimensional structures of proteins. Proteins **17:**355–362.
26. **Tamm, T., and E. Truve.** 2000. Sobemoviruses. J. Virol. **74:**6231–6241.
27. **Tars, K., A. Zeltins, and L. Liljas.** 2003. The three-dimensional structure of cocksfoot mottle virus at 2.7 Å resolution. Virology **310:**287–297.
28. **Terradot, L., M. Souchet, V. Tran, and D. Giblot Ducray-Bourdin.** 2001. Analysis of a three-dimensional structure of Potato leafroll virus coat protein obtained by homology modeling. Virology **286:**72–82.
29. **van Regenmortel, M. H.** 2000. The recognition of proteins and peptides by antibodies. J. Immunoassay **21:**85–108.